



HAL
open science

Wetting and drying scenarios of ionic solutions.

Anna Oleksy, Jean-Pierre Hansen

► **To cite this version:**

Anna Oleksy, Jean-Pierre Hansen. Wetting and drying scenarios of ionic solutions.. *Molecular Physics*, 2011, 109 (07-10), pp.1275-1288. 10.1080/00268976.2011.554903 . hal-00692117

HAL Id: hal-00692117

<https://hal.science/hal-00692117>

Submitted on 28 Apr 2012

HAL is a multi-disciplinary open access archive for the deposit and dissemination of scientific research documents, whether they are published or not. The documents may come from teaching and research institutions in France or abroad, or from public or private research centers.

L'archive ouverte pluridisciplinaire **HAL**, est destinée au dépôt et à la diffusion de documents scientifiques de niveau recherche, publiés ou non, émanant des établissements d'enseignement et de recherche français ou étrangers, des laboratoires publics ou privés.



Wetting and drying scenarios of ionic solutions.

Journal:	<i>Molecular Physics</i>
Manuscript ID:	TMPH-2010-0453.R2
Manuscript Type:	Special Issue paper - In honour of Bob Evans
Date Submitted by the Author:	09-Dec-2010
Complete List of Authors:	Oleksy, Anna; University of Cambridge Hansen, Jean-Pierre; University of Cambridge, Chemistry
Keywords:	wetting, drying, ionic solutes, density functional theory
<p>Note: The following files were submitted by the author for peer review, but cannot be converted to PDF. You must view these files (e.g. movies) online.</p> <p>source files.zip</p>	

SCHOLARONE™
Manuscripts

Wetting and drying scenarios of ionic solutions.

ANNA OLEKSY and JEAN-PIERRE HANSEN

Department of Chemistry, University of Cambridge, Cambridge CB2 1EW (UK)

We review recent theoretical results obtained for the wetting and drying behaviour of ionic solutions near a charged solid substrate. Three levels of modelling ionic solutions are considered: the primitive model, where the solvent is replaced by a dielectric continuum; the "semi-primitive" model where the solvent is represented by hard spheres with a Yukawa attraction and a dielectric permittivity is introduced, which depends on the local solvent density; and the "civilized" model, where the solvent molecules are dipolar hard spheres with a Yukawa attraction. Calculations on the primitive model are based on a square gradient functional for the solvent, combined with a Poisson-Boltzmann description of the ions; the discrete solvent models are treated within a multi-component density functional theory, combining Rosenfeld's fundamental measure description of excluded volume effects with the mean field approximation for the Yukawa and electrostatic interactions. Qualitative agreement is found between the predictions of the three models, while those of the two discrete solvent models agree quantitatively. The relative size of anions and cations is shown to have a crucial influence on interfacial properties, as observed experimentally. A novel drying scenario is predicted near a charged wall. New results are reported for the variation of the surface tension γ with ion concentration c . Contrary to the observed behaviour of aqueous ionic solutions, the liquid/vapour surface tension is found to systematically decrease with c , presumably because our solvent models are insufficient to describe water, due to the neglect of strong hydrogen bonding. The solid/liquid surface tension is in contrast shown to be a non-monotonic function of c and to possess a minimum.

1 Introduction.

Solutes can profoundly modify the interfacial properties, in particular the surface tension γ , of solvents. While surfactants radically reduce the surface tension of water/oil interfaces, ions, on the contrary, lead to a significant increase of the surface tension of the water/air interface [1], which may be traced back to strong Coulombic interactions [2–4]. Since γ , which is the surface excess contribution to the free energy of an inhomogeneous fluid, controls the wetting of a solid (or liquid) substrate by a saturated vapour, or the conjugate drying behaviour of the coexisting liquid phase, it is to be expected that any solute will affect the wetting and drying transitions of the pure solvent. However, while the experimental investigation [5], and theoretical understanding [6] of wetting transitions are well advanced for pure fluids and mixtures, much less attention has been devoted to the study of wetting and drying phenomena of ionic solutions. The reason for this may lie in the complication linked to the additional length scale, the Debye screening length λ_D , which competes with the usual length scales, namely the film thickness ζ , the width δ of the liquid/vapour interface, and the range of the substrate/fluid attraction. λ_D controls the strength of the electrostatic repulsion between the electric double-layers which form at the substrate/fluid and liquid/vapour interfaces, and hence affects the thickness of the liquid wetting film [7–10]. However, the influence of such effects on the wetting and drying scenarios of ionic solutions has only recently been investigated theoretically, within a mean-field framework, using the tools of density functional theory of inhomogeneous fluids [11,12].

In the present paper we review this recent work [13–17], and present some new results on the variation of the substrate/fluid and liquid/vapour surface tensions with ion concentration. After a brief reminder of mean field theories of wetting and drying transitions in simple fluids (Section 2), we introduce the models and approximations used to describe inhomogeneous ionic solutions (Section 3). In Sections 4–6 we present the DFT results obtained with increasingly “realistic” representations of ionic solutions, namely the “primitive” model (Section 4), the “semi-primitive” model (Section 5) and the “civilised” model (Section 6). Our new data concerning the ion concentration dependence of the surface tension are presented in Section 7, while conclusions are drawn in Section 8.

2 Mean field theories of surface phase transitions.

The present discussion will be restricted to three-phase equilibrium between a “spectator phase” *a*, taken here to be a planar solid substrate, and two fluid phases (liquid *b* and vapour *c*). The competition, as a function of temperature and proximity of liquid/vapour coexistence, of the interfacial free energies, or surface tensions γ_{ab} , γ_{ac} and γ_{bc} gives rise to surface phase transitions, namely wetting and drying. If a saturated vapour is put into contact with a solid substrate, which exerts an attractive force on the vapour molecules, a microscopically thin “liquid” film forms at contact. This partial wetting situation is characterised by the thermodynamic inequality:

$$\gamma_{ac} < \gamma_{ab} + \gamma_{bc} \quad (1)$$

and is observed well below the liquid/vapour critical temperature T_c . However, as the temperature is increased along liquid/vapour coexistence, a simple argument due to Cahn [18] shows that at a wetting temperature T_w , the inequality (1) becomes an equality, and a macroscopically thick liquid

1 film intrudes between the substrate and the vapour. This wetting transition is usually first order, i. e.
 2 the liquid film thickness ζ jumps discontinuously from a finite (microscopic) value below T_w (partial
 3 wetting) to infinity (complete wetting). In some rare cases a second order scenario has been observed
 4 [5], where the film thickness diverges continuously as T_w is approached from below (second order or
 5 continuous wetting transition). In the case of a first order wetting transition at T_w , there is an addi-
 6 tional twist, predicted theoretically by Cahn [18], and by Ebner and Saam [19] in 1977, namely a
 7 prewetting transition as vapour/liquid coexistence is approached along an isotherm $T > T_w$ from the
 8 undersaturated vapour side. The film thickness undergoes a finite discontinuity (jump) as a prewetting
 9 line is crossed; after that ζ diverges continuously as the coexistence line is approached. The prewet-
 10 ting line starts on the coexistence curve at $T = T_w$, where the discontinuity is infinite, and moves into
 11 the undersaturated vapour region where the discontinuity remains finite. Its amplitude decreases with
 12 increasing T and vanishes at a prewetting critical point T_{pwc} , above which the film thickness varies
 13 continuously.

14 On the liquid side of the phase diagram, conjugate drying may be observed, where a gas layer
 15 intrudes between the bulk liquid and a solid substrate. The thickness of this “vapour film” increases
 16 continuously as coexistence is approached along an isotherm, and diverges at coexistence [20, 21].

17 The film thickness, or equivalently the adsorption Γ , is the obvious order parameter characteris-
 18 ing the surface phase transitions. If the structureless, impenetrable substrate is taken to be the xy
 19 plane ($z=0$), the local fluid density, or density profile $\rho(z)$ is the fundamental quantity within DFT of
 20 classical inhomogeneous fluids [11, 12]. The adsorption is defined as:

$$21 \Gamma = \int_0^{\infty} [\rho(z) - \rho^{(0)}] dz \quad (2)$$

22 where $\rho^{(0)}$ is the bulk density of the fluid, far from the substrate (i. e. as $z \rightarrow \infty$). The film thickness
 23 ζ may be defined as $\zeta = |\tilde{\Gamma}| = |\Gamma/\rho^{(0)}|$.

24 Within DFT the equilibrium density profile is obtained by minimizing an approximate expression
 25 for the grand potential functional (per unit area of the substrate) $\Omega[\rho(z)]$ with respect to $\rho(z)$, for a
 26 fixed chemical potential μ , namely:

$$27 \Omega[\rho(z)] = F[\rho(z)] + \int_0^{\infty} [V(z) - \mu] \rho(z) dz \quad (3)$$

28 where $F[\rho(z)]$ is an approximate free energy functional (per unit area) and $V(z)$ is the potential of
 29 the force exerted by the substrate on the fluid molecules. The Euler-Lagrange equation leads to the
 30 following generic expression for the density profile [11, 12]:

$$31 \rho(z) = \rho^{(0)} \exp \left\{ -\frac{1}{k_B T} [\mu[\rho(z)] - \mu(\rho^{(0)}) + V(z)] \right\} \quad (4)$$

32 where $\rho^{(0)} = \rho(z \rightarrow \infty)$ is the bulk density,

$$33 \mu[\rho(z)] = \frac{\delta F[\rho(z)]}{\delta \rho(z)} \quad (5)$$

is the “local” chemical potential, and $\mu(\rho^{(0)}) = \mu$ is the overall (bulk) chemical potential. For a given free energy functional F , eq. (4) must be solved iteratively. Substitution of the solution into the surface excess grand potential yields the surface tension γ :

$$\gamma = \Omega^{\text{ex}}[\rho(z)] = \Omega[\rho(z)] - \Omega(\rho^{(0)}) = F[\rho(z)] - F(\rho^{(0)}) + \int_0^\infty V(z)\rho(z)dz - \mu\Gamma \quad (6)$$

Note that the adsorption (2) and the surface tension are related by the Gibbs adsorption equation [11, 12]:

$$\Gamma = - \left(\frac{\partial \gamma}{\partial \mu} \right)_T \quad (7)$$

which provides a useful test of the thermodynamic consistency of results based on approximate functionals [22].

At this stage, one may schematically distinguish between two classes of DFTs of wetting and drying. Following the pioneering work of Cahn [18], phenomenological theories are based on generalisations of van der Waals classic “square gradient” theory of the liquid/vapour interface [12, 23, 24]. Microscopic theories, starting from a molecular description of the fluid, were pioneered by Ebner and Saam [19], and by Sullivan [25, 26], and culminated in the decisive work of Evans and collaborators [21, 27–29]. Following van der Waals, Cahn assumes the density profile $\rho(z)$ to vary slowly near contact. The substrate-fluid interaction is assumed to act only at contact:

$$V(z) = V_0(\rho(z))\delta(z) \quad (8a)$$

with:

$$\frac{V_0(\rho)}{k_B T} = \gamma_0 - \gamma_1 \rho + \frac{1}{2} \gamma_2 \rho^2 \quad (8b)$$

The square gradient expression for the surface excess grand potential hence reads [6, 18]:

$$\frac{\Omega^{\text{ex}}[\rho(z)]}{k_B T} = \int_0^\infty \left\{ W(\rho(z)) + \frac{B}{2} \left[\frac{d\rho(z)}{dz} \right]^2 \right\} dz + \gamma_0 - \gamma_1 \rho_s + \frac{1}{2} \gamma_2 \rho_s^2 \quad (9)$$

where $\rho_s = \rho(z=0)$ is the contact value of the local density. $W(\rho)$ is the reduced bulk grand potential density (local density approximation), while the coefficient $B/2$ of the non-local square gradient correction is assumed to be independent of density. In the vicinity of the critical point $W(\rho)$ may be approximated by the double well form:

$$W(\rho) = c(\rho - \rho_l)^2(\rho - \rho_v)^2 \quad (10)$$

where ρ_l and ρ_v are the temperature-dependent densities of the coexisting liquid and vapour phases, and c is another phenomenological coefficient. The equilibrium profile is easily calculated to be:

$$\rho(z) = \rho_v + \frac{(\rho_l - \rho_v)}{1 + \exp[(z - \zeta)/\delta]} \quad (11)$$

where $\delta = \sqrt{B/2c}(\rho_1 - \rho_v)^{-1}$ is the van der Waals width of the liquid/vapour interface [12, 23, 24], and $\zeta = -\delta \ln C = -\delta \ln [(\rho_1 - \rho_s)/(\rho_s - \rho_v)]$ is the film thickness. Substitution of (11) into (9) yields the reduced surface excess grand potential in the form [13, 14]:

$$\frac{\Omega^{\text{ex}}}{k_B T} \equiv \omega^{\text{ex}} = \omega_0^{\text{ex}} + 6\gamma \left[\frac{1}{2(1+C)^2} - \frac{1}{3(1+C)^3} - \frac{1}{6} + (p_1 - p_2) \frac{C}{1+C} + \frac{1}{2} p_2 \left(\frac{C}{1+C} \right)^2 \right] \quad (12)$$

where $\omega_0^{\text{ex}} = \gamma + \gamma_0 - \gamma_1 \rho_1 + \frac{\gamma_2}{2} \rho_1^2$, $\gamma = \sqrt{2Bc}(\rho_1 - \rho_v)^3/6$ is the van der Waals surface tension of the liquid/vapour interface, and p_1 and p_2 are the two control parameters

$$p_1 = \frac{\gamma_1}{\sqrt{2Bc}}(\rho_1 - \rho_v)^2; \quad p_2 = \frac{\gamma_2}{\sqrt{2Bc}}(\rho_1 - \rho_v)^{-1} \quad (13)$$

ω^{ex} is finally minimised with respect to C (or equivalently to the contact density ρ_s), which determines the film thickness ζ corresponding to the lowest minimum of ω^{ex} for any given temperature (i. e. ρ_1 and ρ_v). Depending on the values of the two control parameters p_1 and p_2 , a first (discontinuous) or second order wetting transition is predicted along the liquid/vapour coexistence curve. The Cahn theory also predicts the prewetting scenario as the coexistence curve is approached from the undersaturated vapour side, provided the grand potential density (10) is generalised to incorporate an additional contribution linear in $(\rho - \rho_v)$ proportional to the degree of undersaturation [14, 18]. Cahn's theory is very attractive because of its fully analytic nature, but it requires a large number of thermodynamic or phenomenological parameters as input ($\rho_1(T)$, $\rho_v(T)$, B , c , γ_1 , γ_2) which must be taken from a separate microscopic theoretical description, or from experiment.

Microscopic density functional theories are based on a molecular model of the fluid, which specifies the Hamiltonian of the system, i. e. the interactions between the molecules [19, 21, 25–29]. Following van der Waals, the pair potential is split into a short-range repulsion and long-range (LR) contributions (dispersion and Coulombic interactions). The former is conveniently taken to be of the simple hard sphere (HS) form. Accordingly, the free energy functional $F[\rho]$ may be split into ideal, HS and LR contributions:

$$F[\rho(z)] = F_{\text{id}}[\rho(z)] + F_{\text{HS}}[\rho(z)] + F_{\text{LR}}[\rho(z)] \quad (14)$$

While $F_{\text{id}}[\rho(z)]$ is known exactly [11, 12]

$$F_{\text{id}}[\rho(z)] = k_B T \int_0^\infty \rho(z) \{ \log(\Lambda^3 \rho(z)) - 1 \} dz \quad (15)$$

approximate expressions must be used for the contributions F_{HS} and F_{LR} due to intermolecular forces. Weighted density approximations have been used for F_{HS} by the Bristol group [21, 27–29], but the work on ionic solutions reported in the following Sections is based on the more accurate “fundamental measure” functional introduced by Rosenfeld [30] in its most refined form [31, 32]. The long-range contribution to the free energy is almost invariably taken to be of the non-local mean-field form:

$$F_{\text{LR}}[\rho(z)] = \frac{1}{2} \int_0^\infty dz \int_0^\infty dz' \rho(z) w(|z - z'|) \rho(z') \quad (16)$$

where w is the long-range part of the pair potential, suitably integrated over the transverse (x, y) coordinates.

Minimisation of the corresponding grand potential (3) with respect to $\rho(z)$ can no longer be carried out analytically but requires careful iterative numerical solutions [21, 27–29]. The various wetting scenarios predicted by Cahn’s phenomenological theory are confirmed by the “first principles” DFT approach. A key finding of the Bristol group is that the order of the wetting transition is very sensitive to the range of the substrate/fluid attraction, relative to that of the attractive potential $w(z)$ between fluid molecules. Short-range substrate/fluid attractions favour a continuous wetting transition, while first order wetting and prewetting transitions are found to occur when the range of the attraction exerted by the substrate on the fluid molecules exceeds a threshold [27].

In the following Sections the phenomenological and microscopic DFT approaches are generalised to the case of simple models of ionic solutions [13–17]. It is important to stress at the outset that for any theory of wetting or drying to be consistent, the interfacial and bulk thermodynamic properties must be calculated throughout from the SAME free energy functional, which reduces to a function of the constant densities in the bulk.

3 Simple models of ionic solutions.

Ionic solutions are (at least) three-component systems involving the solvent, cations and anions. To investigate their interfacial properties next to a neutral or charged planar substrate, one must introduce three density profiles $\rho_0(z)$ (solvent), $\rho_+(z)$ and $\rho_-(z)$. A fundamental combination of the latter two profiles is the local charge density:

$$\rho_c(z) = \sum_{\alpha=+,-} q_\alpha \rho_\alpha(z) \quad (17)$$

where q_α is the charge carried by ionic species α . The profiles determine the partial adsorptions of the three species:

$$\Gamma_\alpha = \int_0^\infty dz [\rho_\alpha(z) - \rho_\alpha^{(0)}] \quad (18)$$

which are in turn related to the interfacial tension γ by the generalisation of the Gibbs adsorption equation (7):

$$\Gamma_\alpha = - \left(\frac{\partial \gamma}{\partial \mu_\alpha} \right)_{T, \{\mu_\beta\}} \quad (19)$$

Through their long-range Coulombic interaction and the requirement of charge neutrality, both globally, and locally through the screening mechanism, the ions introduce qualitatively different interfacial behaviour (compared to the pure solvent), essentially through the formation of electric double-layers at the substrate/fluid and liquid/vapour interfaces. We have studied how the ions modify the wetting and drying behaviour of the pure solvent, using three different models of the ionic solution:

- a) The “primitive” model, where ions and solvent molecules are completely decoupled, the solvent playing only the role of a dielectric continuum of fixed permittivity ϵ relative to the ions. The

phenomenological theory combines Cahn's theory for the solvent as sketched in Section 2, with Poisson-Boltzmann theory for the inhomogeneous "fluid" of ions. This Cahn-Poisson-Boltzmann approach [13, 14] will be presented in Section 4.

- b) The "semi-primitive" model (SPM) takes the molecular granularity of the solvent explicitly into account, by representing the solvent molecules by neutral hard spheres with attractive interactions between all solvent-solvent, solvent-ion and ion-ion pairs; the ions are charged hard spheres. Since the model ignores the polar nature of the solvent molecules, it must be supplemented by the introduction of a local dielectric permittivity $\varepsilon(z)$ depending on the local solvent density to allow for solute dissociation [15, 16]. This model will be considered in Section 5.
- c) The "civilized" model [33,34] introduces an explicitly polar solvent, by representing its molecules by dipolar hard spheres. Apart from this crucial refinement, the model is similar to the SPM, but does not require the phenomenological introduction of a local permittivity $\varepsilon(z)$, since the dielectric properties of the solvent are now controlled by its molecular dipolar moment. The wetting and drying behaviour of the "civilized" model [17] will be the subject of Section 6.

4 The primitive model: Cahn-Poisson-Boltzmann theory.

Within the primitive model, the surface excess grand potential is assumed to be the sum of two independent contributions, both functions of the film thickness ζ ; the solvent contribution Ω^s , derived from Cahn's square gradient theory (cf. eq. (9)), and an electrostatic contribution Ω^{el} due to the electric double-layers formed by the ions at the substrate/liquid and liquid/vapour interfaces; the latter is calculated within the non-linear Poisson-Boltzmann (PB) theory of ions in a continuous solvent of dielectric permittivity ε .

$$\Omega^{ex}(\zeta) = \Omega^s(\zeta) + \Omega^{el}(\zeta) \quad (20)$$

The substrate carries a uniform surface charge chosen to be negative for clarity, $\sigma = -q/a$, where a is the area per unit charge. The counterions carry a charge $+q$, while the coions have a charge $-q$ (symmetric electrolyte). The generalisation to ions of different valences is straightforward. The cation and anion density profiles within the wetting film satisfy Poisson's equation:

$$\frac{d^2\Phi(z)}{dz^2} = -4\pi l_B [\rho_+(z) - \rho_-(z)] \quad (21)$$

where $\Phi(z)$ is the dimensionless electrostatic potential $q\Psi(z)/k_B T$ and $l_B = q^2/(\varepsilon k_B T)$ is the Bjerrum length.

Assuming the ion concentration in the vapour phase above the liquid film to be negligible (i. e. ions do not leak outside the film), the potential must satisfy the boundary conditions:

$$\left. \frac{d\Phi(z)}{dz} \right|_{z=0} = -\frac{4\pi l_B}{a}; \quad \left. \frac{d\Phi(z)}{dz} \right|_{z=\zeta} = 0 \quad (22)$$

which are equivalent to the overall charge neutrality condition:

$$\int_0^\zeta [\rho_+(z) - \rho_-(z)] dz = \frac{1}{a} \quad (23)$$

The PB free energy functional is the sum of ideal and mean field electrostatic contributions:

$$f^e = \frac{F^e}{Ak_B T} = \sum_{\alpha=\pm} \int_0^\zeta \rho_\alpha(z) [\log(\Lambda_\alpha^3 \rho_\alpha(z)) - 1] dz + \frac{1}{2} \int_0^\zeta \rho_c(z) \Phi(z) dz \quad (24)$$

where $\rho_c(z) = \rho_+(z) - \rho_-(z) - \delta(z)/a$ is the total charge density (in units of q).

Imposing chemical equilibrium throughout the wetting film:

$$\mu_\alpha(z) = \frac{\delta f^e [\{\rho_\beta(z)\}]}{\delta \rho_\alpha(z)} = \mu^{(0)} \quad (25)$$

where $\mu^{(0)}$ is the bulk chemical potential of anions and cations, the Boltzmann form of the density profiles is recovered:

$$\rho_\pm(z) = \rho^{(0)} \exp\{\mp \Phi(z)\} \quad (26)$$

Substitution of (26) back into eq. (21) results in the PB equation:

$$\frac{d^2 \Phi(z)}{dz^2} = 8\pi l_B \rho^{(0)} \sinh(\Phi(z)) \quad (27)$$

which must be solved, for a given film thickness ζ , subject to the boundary conditions (22). This can be achieved analytically, in parametric form [13, 14]. The solution may be substituted in the free energy functional (24) to yield an analytic expression for the electrolyte contribution to the surface excess grand potential:

$$\omega^e = \frac{\Omega^e}{Ak_B T} = f^e - \mu^{(0)} \int_0^\zeta [\rho_+(z) + \rho_-(z)] dz \quad (28)$$

as a function of the film thickness ζ . Gathering the results for the pure solvent (eq. (12)) and for the electrolyte, one obtains the total surface excess grand potential as a function of ζ . The following scenarios emerge:

- a) In the simple case where only counterions (released by the substrate into the film upon ionisation) are present (i. e. $\rho_-(z) \equiv 0$), the electrostatic contribution ω^e is always positive, and decays like $1/\zeta$ due to the lack of screening, while the solvent contribution ω^s decays exponentially with ζ . Consequently the variation of $\omega^{\text{ex}} = \omega^s + \omega^e$ with film thickness is dominated by ω^e as $z \rightarrow \infty$, and the wetting transition will always be first order, irrespective of the discontinuous (first order) or continuous (second order) nature of the wetting transition of the pure solvent [13, 14].
- b) In the more general case of added salt (i. e. the presence of counterions and coions), the wetting behaviour is controlled by three dimensionless parameters, in addition to the parameters p_1 and p_2 , defined in eq. (13), which control the wetting scenarios of the pure solvent; these three parameters are determined by the two additional physical variables, namely the reservoir chemical potential $\mu^{(0)}$, or equivalently the reservoir ion concentrations $\rho_+^{(0)} = \rho_-^{(0)} = \rho^{(0)}$ (symmetric electrolyte) and the surface charge density $\sigma = q/a$ (the three parameters are hence not fully independent). They are:

$$\bar{\delta} = \kappa_D \delta; \quad \eta = \frac{\rho^{(0)}}{3\kappa_D \gamma}; \quad K = \frac{4\pi l_b}{a\kappa_D} \quad (29)$$

where δ and γ are the liquid/vapour interfacial width and reduced surface tension of the pure solvent defined after eqs. (11) and (12), while $\kappa_D = \sqrt{8\pi\rho^{(0)}l_B}$ is the inverse Debye screening length.

When salt is present ($\rho^{(0)} \neq 0$), the electrostatic interactions are screened, and the wetting transition of the ionic solution may be either continuous or discontinuous, depending on the specific values of $\rho^{(0)}$ and σ . When $\rho^{(0)} \neq 0$, ω^e decays exponentially with $\bar{\zeta} = \kappa_D\zeta$. The wetting transition is always discontinuous (as for the salt-free case) as long as $\rho^{(0)} < \bar{\rho}^{(0)} \simeq 0.05\text{M}$ [14]. When $\rho^{(0)} > \bar{\rho}^{(0)}$, three different wetting scenarios may occur [14]:

- (i) Upon increasing the solvent control parameter p_1 , a discontinuous wetting transition occurs at some $p_1^{\text{tr}} > p_2$.
- (ii) As p_1 is increased, a continuous wetting transition occurs at $p_1^{\text{tr}} = p_2$.
- (iii) A succession of two wetting transitions is observed: first a discontinuous jump between a smaller value ζ_1^{tr} and a larger value ζ_2^{tr} of the film thickness occurs at some $p_1^{\text{tr}} < p_2$; this discontinuous transition is followed by a continuous divergence of ζ as $p_1 \rightarrow p_2$. Unlike in the case of prewetting, this sequence of wetting transitions is observed along the vapour/liquid coexistence curve, with the continuous transition occurring close to the critical point; this scenario is a direct consequence of the appearance of two minima in the total surface excess grand potential ω as a function of ζ .

For high salt concentrations $\rho^{(0)}$ the electrostatic forces are strongly screened, and do not change the order of the wetting transition of the pure solvent.

The various scenarios may be understood in terms of the competition of two different length scales in the ionic solution - the bulk correlation length δ of the solvent and the Debye screening length κ_D^{-1} . Maps of the occurrence of the wetting scenarios in parameter space are given in ref. [14]. In the case of aqueous ionic solutions the wetting behaviour is expected to be very similar to that of pure water due to its very high surface tension γ . Interesting effects may be observable for weakly polar solvents (with $\gamma \ll \gamma_{\text{H}_2\text{O}}$) or in the presence of organic surfactants.

5 The semi-primitive model

The phenomenological Cahn-PB theory of wetting by ionic solutions has some obvious limitations: the underlying “primitive” model ignores the coupling between ions and solvent; the square-gradient and PB approximations cannot account for the strong layering of solvent molecules and ions near the substrate, due to excluded volume effects; the free energy functional is not directly related to an underlying microscopic model of the solution, and requires the input of a number of phenomenological parameters, which must be taken from experiment or independent theoretical calculations, e. g. of the liquid/vapour phase diagram. A more microscopic approach, based on a well defined Hamiltonian, is clearly desirable. This would be a formidable task for realistic models of water, but simplified models of the solvent may be expected to provide at least a qualitative picture of the influence of dissolved ions on the wetting and drying behaviour of the solvent, which may be confronted with the trends predicted in Section 4 on the basis of Cahn-PB theory.

The “semi-primitive” model (SPM) briefly introduced in Section 3 is a step in that direction. Solvent molecules are taken to be neutral hard spheres of diameter d_0 , while cations and anions are charged hard spheres of diameters d_+ and d_- ; the investigations in reference [16] are restricted to monovalent ions ($q_+ = +e$, $q_- = -e$), and the diameters taken equal to their Pauling values. This is the basic model examined in ref. [15]. The Coulombic interactions between ions are reduced by a constant permittivity ε associated with the solvent, hence the name of “semi-primitive” model; it takes into account the granularity of the solvent (unlike the “primitive” model), but its polar nature is accounted for only on a macroscopic level, as is the case with the dielectric continuum representation of the “primitive” model.

Ion and solvent density profiles and related interfacial properties of the SPM near a neutral or charged hard wall were calculated in ref. [15] on the basis of a free energy functional detailed below including an approximate Coulomb correlation term [35], for NaCl, KCl and CaCl₂. For the monovalent ion cases and moderate surface charges σ the correlation term does not significantly modify the predictions based on the mean-field density functional, which yields density profiles in reasonable agreement with Monte Carlo data for a symmetric SPM [15, 36].

Wetting and drying phenomena being controlled by cohesive substrate/fluid and fluid/fluid forces, the above SPM must be augmented by the addition of attractive interactions between the solvent molecules and the ions, and between the substrate and the solution. Following the work of Sullivan [25, 26] and of Evans and coworkers [21, 27–29], Yukawa-like attractions between all species are assumed. The pair potentials are hence chosen of the generic form ($\alpha, \beta = 0, +, -$):

$$v_{\alpha\beta}(r) = \begin{cases} \infty; & r < d_{\alpha\beta} = (d_\alpha + d_\beta)/2 \\ \frac{q_\alpha q_\beta}{\varepsilon r} - \frac{u}{r} \exp[-k_f(r/d_{\alpha\beta} - 1)]; & r > d_{\alpha\beta} \end{cases} \quad (30)$$

where ε is the (local) dielectric permittivity of the solvent, u is the energy scale (multiplied by unit length) of the attractive interaction, and k_f controls its range. For simplicity u and k_f are assumed to be the same for all $\alpha\beta$ pairs.

The external potential exerted by the planar substrate with surface charge σ on particles of species α is of the form:

$$V_\alpha(z) = \begin{cases} \infty; & z < \frac{1}{2}d_\alpha \\ -u_w \exp\{-k_w(z/d_\alpha - 1)\} - \frac{2\pi\sigma q_\alpha}{\varepsilon(z)}z; & z > \frac{1}{2}d_\alpha \end{cases} \quad (31)$$

where z is the distance from the substrate (xy plane); u_w is the energy scale of the non-Coulombic substrate/solution attraction, while k_w controls its range. Convenient reduced variables are $T^* = k_B T d_0 / u$, $\rho_\alpha^* = \rho_\alpha d_0^3$ and $\sigma^* = \sigma d_0^2 / e$. We know from the work of Tarazona and Evans [27] that the ratio k_f/k_w controls the order of the wetting transition of the pure solvent.

The total free energy functional per unit area, generalising the pure solvent form (14), may be conveniently split into the following contributions:

$$F[\{\rho_\alpha(z)\}] = F_{id}[\{\rho_\alpha(z)\}] + F_{HS}[\{\rho_\alpha(z)\}] + F_Y[\{\rho_\alpha(z)\}] + F_{el}[\{\rho_\alpha(z)\}] \quad (32)$$

The ideal term F_{id} is the sum of three contributions of the form (15). For the hard sphere term we have used the most accurate fundamental measure form adapted to a three-component HS mixture

[15, 32]. For the Yukawa attraction term F_Y and the electrostatic term F_{el} the mean-field form is adopted:

$$F_Y[\{\rho_\alpha(z)\}] = \frac{1}{2} \sum_{\alpha,\beta} \int_0^\infty dz \int_0^\infty dz' \rho_\alpha(z) v_{\alpha\beta}^Y(|z-z'|) \rho_\beta(z') \quad (33)$$

where, using cylindrical coordinates:

$$v_{\alpha\beta}^Y(|z-z'|) = \int_0^{2\pi} d\phi \int_{d_{\alpha\beta}}^\infty r dr v_{\alpha\beta}^Y(|\vec{r}-\vec{r}'|) \quad (34)$$

and

$$F_{el}[\{\rho_\alpha(z)\}] = \frac{1}{2} \int_0^\infty dz \rho_c(z) \Psi(z) \quad (35)$$

where $\rho_c(z)$ is the charge density (17), while $\Psi(z)$ is the local electrostatic potential, which satisfies Poisson's equation:

$$\frac{d}{dz} \left(\varepsilon(z) \frac{d}{dz} \Psi(z) \right) = -4\pi \rho_c(z) \quad (36)$$

Short-range correlations due to excluded volume effects are properly included in the functional (32) through the fundamental measure HS term. Correlations due to the attractive Yukawa interactions and to the long-range Coulombic forces are neglected in the mean-field approximations (33) and (35), but it was shown in ref. [15] that this is a reasonable approximation for the Coulombic term, at least for monovalent ions and moderate surface charges σ .

Three different choices for the local dielectric permittivity $\varepsilon(z)$ have been made in ref. [16]:

- A constant value, equal to the bulk permittivity of the solvent.
- A local Clausius-Mossotti (CM) expression

$$\varepsilon(z) = \frac{1 + \frac{8\pi}{9k_B T} m^2 \tilde{\rho}_0(z)}{1 - \frac{4\pi}{9k_B T} m^2 \tilde{\rho}_0(z)} \quad (37)$$

where m is the assumed dipole moment of the solvent molecules, while $\tilde{\rho}_0(z)$ is the local density of the solvent, averaged over a sphere of diameter d_0 (weighted density).

- A phenomenological, sigmoidal function of the weighted local density, mimicking the permittivity of water [16].

The CM approximation (37) results from a mean-field description of the genuine polar HS solvent used in the "civilized" model considered in Section 6. It is afflicted by the familiar "dielectric catastrophe" at high solvent density, and must hence be restricted to sufficiently small dipole moment m . In the calculations of reference [16] the reduced dipole moment $m^* = m / (ud_0^2)^{1/2}$ was set at $m^* = 0.75$, thus avoiding the "dielectric catastrophe" throughout the fluid range, and yielding dielectric permittivities ε between 5 and 10 in the dense liquid phase (weakly polar solvent).

For a given $\varepsilon(z)$ Poisson's equation (36) was solved numerically by a Runge-Kutta method, subject to the boundary conditions:

$$\left. \frac{d\Psi(z)}{dz} \right|_{z=0} = -\frac{4\pi\sigma}{\varepsilon(0)}, \quad \frac{d\Psi(z)}{dz} \xrightarrow{z \rightarrow \infty} 0 \quad (38)$$

The equilibrium density profiles are determined by minimizing the grand potential per unit area:

$$\Omega[\{\rho_\alpha(z)\}] = F[\{\rho_\alpha(z)\}] + \sum_\alpha \int_0^\infty dz [V_\alpha(z) - \mu_\alpha] \rho_\alpha(z) \quad (39)$$

with respect to the $\rho_\alpha(z)$ for fixed chemical potentials μ_α . The surface tension γ is finally given by the three-component generalisation of eq. (6).

The liquid/vapour binodal line of the pure solvent and at finite salt concentrations is calculated from the bulk limit ($\rho_\alpha(z) \rightarrow \rho_\alpha^{(0)}$) of the free energy (32). Note that in the mean-field approximation F_{el} vanishes in that limit due to global charge neutrality. The effect of the ions on the phase diagram is hence only due to their contributions to the other terms in the free energy. Up to ion concentrations of 2M this effect is small, and only leads to a modest decrease (1%) of the critical temperature T_c [16]. Inclusion of correlation terms in the Coulombic contributions to the free energy, e.g. within the mean spherical approximation [37], might lead to more substantial changes in the phase diagram, but would spoil thermodynamic self-consistency at the level of the Gibbs adsorption equation (19).

The equilibrium density profiles of the liquid film which forms upon approaching the binodal from the vapour side along an isotherm exhibits strong layering, as illustrated in Fig. 1. As expected the film thickness grows as coexistence is approached, and diverges above a wetting temperature T_w . A second order scenario is observed when the ranges of the wall/fluid and fluid/fluid attractions are comparable. The case $k_w = k_f = 1.8$ is illustrated in Fig. 2. The distance from coexistence is measured as a difference in the Gibbs function $g = \sum_\alpha x_\alpha \mu_\alpha$ (where x_α is the molar fraction of species α) between undersaturated and saturated vapour. When the range of the wall/fluid attraction increases relative to the fluid/fluid attraction, the wetting transition goes over to a discontinuous scenario: prewetting is observed off coexistence, followed by a continuous divergence of the film thickness as coexistence is approached; the case with $k_w = 1.2$, $k_f = 1.8$ is illustrated in Fig. 3.

Concerning the key question of the present investigation, namely the change in the wetting and drying behaviour of the pure solvent induced by the ionic solute, the main conclusions of ref. [16] may be summarised as follows, in terms of two additional physical variables, the salt concentration c and the surface charge density σ . Higher c results in stronger screening of the electrostatic forces, rendering wetting a priori less favourable. The addition of salt is indeed found to generally increase the wetting temperature T_w compared to that of the pure solvent; the effect increases with c and can be as large as 4% for $c=1M$, depending on the assumed permittivity ϵ . On the other hand, for a given c , T_w is found to decrease linearly with $|\sigma|$ if the wetting transition of the pure solvent is first order. Conversely, the variation of T_w is non-monotonic, and depends moreover on the sign of σ when the pure solvent undergoes a second order wetting transition.

The order of the wetting transition in most ionic solutions is predicted to be the same as in the corresponding solute-free fluids. However, in concentrated solutions (short Debye length), where the excess of counterions extends only over roughly one layer, a transition which was continuous in the ion-free solvent may become first order in contact with a highly charged substrate. By contrast, at low salt concentrations (large Debye length), where charge separation near the wall can span the entire width of the liquid film, discontinuous wetting is favoured even for moderate values of $|\sigma|$. These predictions are in overall qualitative agreement with those of the Cahn-PB theory of Section 4. Quantitative comparison is difficult because of the phenomenological nature of the latter, and because

1 the primitive model cannot account for layering effects, which play a subtle role in determining the
2 interfacial behaviour predicted by the explicit solvent model. The work based on the SPM found
3 no evidence of the sequence of two wetting transitions along the coexistence curve predicted in ref.
4 [14] (Section 4) for some ionic solutions in the region of parameter space adjacent to that where the
5 crossover from a discontinuous to a continuous transition takes place. The scenario cannot be com-
6 pletely ruled out, since the fraction of parameter space explored in ref. [16] is much smaller than in
7 ref. [14] due to the much larger computational effort required with the explicit solvent model.

8 When the liquid/vapour coexistence curve is approached from the liquid side along an isotherm,
9 drying (or dewetting) is commonly observed near a solid substrate if $u_w = 0$. The solute-free HCY
10 solvent was shown to dry completely in contact with a hard wall, i. e. an infinitely thick vapour layer
11 intrudes between the liquid and the substrate for any temperature between the triple and critical points
12 [16]. When ions and surface charge on the substrate are added, the drying behaviour of the system
13 changes radically due to the Coulombic interaction between the electric double layers which form at
14 the fluid/substrate and liquid/vapour interfaces. The monovalent counterions are strongly attracted to
15 the oppositely charged substrate, where they form an adsorbed layer, which only partially neutral-
16 izes the surface charge, while the Cl^- ions outnumber the Na^+ cations at the liquid/vapour interface,
17 which is hence negatively charged, in agreement with experimental observations [38] and molecular
18 dynamics simulations [39,40] of aqueous solutions. The situation is illustrated by the density profiles
19 calculated at liquid/vapour coexistence for $\sigma > 0$ (Fig. 4) and for $\sigma < 0$ (Fig. 5). When $\sigma > 0$ the two
20 interfaces attract each other because the electric double-layers carry opposite charges; this attraction
21 hinders complete drying which is only observed when $\sigma \rightarrow 0$. When $\sigma < 0$, cations are preferentially
22 adsorbed on the substrate, but the corresponding double-layer charge remains globally negative, thus
23 repelling the negatively charged liquid/vapour interface, and favouring drying. Complete drying is
24 indeed predicted for $|\sigma|$ less than a threshold value (of the order of $1e/\text{nm}^2$, the precise value de-
25 pends on the concentration and temperature of the solution). But drying can be hindered if $|\sigma|$ is
26 sufficiently large for the Yukawa attraction between the adsorbed cations and the solvent to outweigh
27 the solvent-solvent cohesion forces and the electrostatic repulsion between the two interfaces. For a
28 fixed moderate value of $|\sigma|$ the calculations of ref. [16] predict a first order drying transition between
29 a partially wet wall (finite film thickness) and a completely dry wall above a drying temperature T_d
30 along the liquid/vapour coexistence curve. Contrary to the conjugate wetting temperature T_w , T_d is
31 found to increase with $|\sigma|$. For very low values of $|\sigma|$, T_d lies below the triple point, and the wall is
32 completely dry for any thermodynamic state on the binodal. Conversely, if the substrate carries a very
33 large negative charge density $T_d > T_c$ and the wall is always partially wet. Analogously to wetting,
34 pre-drying is observed upon approaching the liquid/vapour coexistence curve along an isotherm above
35 T_d . The first order drying transition is predicted to occur in the absence of any wall/liquid dispersion
36 attraction. It would be interesting to investigate the competition between substrate/fluid Coulombic
37 and dispersion forces.

51 52 53 6 The “civilized” model.

54 In a further step towards physical reality the “civilized” model, featuring a dipolar solvent was used
55 in ref. [17] to investigate the wetting and drying behaviour of ionic solutions. The solvent molecules
56 are HCY spheres carrying a dipole moment \vec{m}_0 . Charge-dipole and dipole-dipole contributions must
57
58
59
60

be added to the pair potentials (30), namely:

$$V_{\alpha\beta}^d(\vec{r}, \vec{m}_\alpha, \vec{m}_\beta) = \frac{1}{r^3} q_\alpha \vec{m}_\beta \cdot \vec{r} - \frac{m_\alpha m_\beta}{r^3} [3(\hat{m}_\alpha \cdot \hat{r})(\hat{m}_\beta \cdot \hat{r}) - \hat{m}_\alpha \cdot \hat{m}_\beta] \quad (40)$$

where $\vec{m}_\alpha = \vec{0}$ for $\alpha \neq 0$, while $q_\alpha = 0$ for $\alpha = 0$. The external potential acting on the polar molecules is now:

$$V_0(z, \theta) = \begin{cases} \infty, & z < \frac{1}{2}d_0 \\ -u_w \exp\{-k_w(z/d_0 - 1)\} - 2\pi\sigma m_0 \cos(\theta) \end{cases} \quad (41)$$

where θ is the polar angle of \vec{m}_0 relative to the z axis (normal to the substrate).

The density profile of the solvent depends on the local orientation of the dipole:

$$\rho(z, \theta) = \rho(z)\alpha(z, \theta) \quad (42)$$

where $\alpha(z, \theta)$ may be expanded in Legendre polynomials:

$$\alpha(z, \theta) = \sum_{l=0}^{\infty} \alpha_l(z) P_l(\cos(\theta)) \quad (43)$$

with $\alpha_0(z) = 1/4\pi$ for proper normalization.

Consider first the solute-free pure solvent, placed inside a condenser of oppositely charged plates ($\pm\sigma$, to ensure overall charge neutrality in the absence of ions). The free energy functional $F[\rho_0(z, \theta)]$ may be split into ideal, hard sphere, Yukawa and electrostatic contributions, as in eq. (32), with (temporarily dropping the subscript 0)

$$\frac{F_{id}[\rho(z, \theta)]}{k_B T} = \int_0^\infty dz \rho(z) \{ \log[\Lambda^3 \rho(z)] - 1 \} + 2\pi \int_0^\infty dz \rho(z) \int_0^\pi d\theta \sin(\theta) \alpha(z, \theta) \log[4\pi \alpha(z, \theta)] \quad (44)$$

The hard sphere contribution F_{HS} is given by the one-component version of the Rosenfeld functional [30, 31], the Yukawa contribution is given by the one-component version of (33), while the electrostatic contribution is, within the mean-field approximation:

$$F_{el}[\rho(z, \theta)] = -\frac{1}{2} \int_0^\infty P(z) E_{dd}(z) dz \quad (45)$$

where $P(z)$ is the local polarization density:

$$P(z) = 2\pi \int_0^\pi m \cos(\theta) \rho(z, \theta) \sin(\theta) d\theta = \frac{4\pi m}{3} \rho(z) \alpha_1(z) \quad (46)$$

while $E_{dd}(z)$ is the local electric field generated by the dipolar particles:

$$E_{dd}(z) = 2\pi \int_0^\infty dz' \left[\frac{|z - z'|^2}{d^3} - \frac{1}{d} \right] P(z') \Theta_H(d - |z - z'|) \quad (47)$$

Θ_H being the Heaviside step function.

The orientation-independent density $\rho(z)$ and the orientational order parameter $\alpha_1(z)$ (and hence the polarization (46)) are determined self-consistently from the Euler-Lagrange equation derived from the minimization of the grand potential functional (3) of $\rho(z, \theta)$ [17]. Due to the mean-field approximation for F_{el} the orientational order parameter takes the classic Langevin form:

$$\alpha_1(z) = \frac{3}{4\pi} \left[\coth(\beta m E(z)) - \frac{1}{\beta m E(z)} \right] \quad (48)$$

where $E(z) = E_0 + E_{dd}(z) = 2\pi\sigma + E_{dd}(z)$ is the total electric field acting on the dipoles. For the same reason the dielectric permittivity of the bulk dipolar solvent reduces to the classic Clausius-Mossotti form, the local version (37) of which was used in the SPM description of Section 5. To avoid the “dielectric catastrophe”, all DFT calculations are restricted to a reduced dipole moment $m^* = \sqrt{m/ud^3} \leq 0.9$.

For $\sigma = 0$ the model reduces to the HCY solvent model of Section 5; when $\sigma \neq 0$ the electric field partly orients the dipole moments, and this leads to a drop of the critical temperature T_c proportional to m^* [17]. Note that if dipole-dipole correlations are taken into account [41, 42], T_c of the non-electrified ($\sigma = 0$) polar solvent increases with m^* . Detailed DFT calculations [17] show that the wetting scenarios of the dipolar solvent are very similar to those of the HCY solvent ($m^* = 0$). The wetting temperature T_w drops as m^* increases from 0 (HCY limit) for fixed values of σ , but the ratio T_w/T_c is practically independent of σ and m^* , both for first and second order transitions.

When ions are added the DFT calculations very much proceed as for the SPM in Section 5, except that the local electric potential $\Psi(z)$ now satisfies Poisson’s equation:

$$\frac{d^2\Psi(z)}{dz^2} = -4\pi\rho_c(z) + 4\pi\frac{dP(z)}{dz} \quad (49)$$

rather than eq. (36). As illustrated in Fig. 6, the density profiles calculated for the “civilized” model are practically indistinguishable from those obtained for the SPM under identical physical conditions (T, c, m^*), provided the local CM permittivity (37) is used in the SPM calculations. This remarkable agreement seems to be the first justification of the use of a local dielectric permittivity $\varepsilon(z)$ in the description of inhomogeneous ionic solutions (in particular in explicit solvent descriptions of electric double layers), at least within a mean-field context.

A direct consequence of this close agreement between the density profiles, and hence the adsorptions Γ_α predicted by the two models, is that the wetting and drying scenarios of the “civilized” model are qualitatively and quantitatively identical to those described in Section 5 for the SPM. In particular the novel drying transitions predicted in Section 5 are confirmed by the DFT calculations based on the “civilized” model [17].

7 Surface tension.

In this section we focus on the surface tension of liquid/vapour and solid/fluid interfaces of the three-component explicit solvent models of ionic solutions discussed above. In particular, we investigate the influence of ion concentration and distribution (electric double-layers) on interfacial tension. Within

DFT the surface tension is a functional of the equilibrium density profiles of the species present in the system. A generalization of eq.(6) appropriate to describe the free liquid/vapour interface is:

$$\gamma_{lv} = F [\{\rho_{\alpha}(z)\}] - F [\{\rho_{\alpha}^{SK}(z)\}] - \sum_{\alpha} \int_{-\infty}^{\infty} \mu_{\alpha} (\rho_{\alpha}(z) - \rho_{\alpha}^{SK}(z)) dz \quad (50)$$

where $\rho_{\alpha}^{SK}(z)$ are sharp-kink density profiles:

$$\rho_{\alpha}^{SK}(z) = \begin{cases} \rho_{\alpha}^{SK}(z) = \rho_{\alpha}^v, & z < 0 \\ \rho_{\alpha}^{SK}(z) = \rho_{\alpha}^l, & z > 0 \end{cases} \quad (51)$$

while ρ_{α}^v and ρ_{α}^l are the densities of species α in the vapour and in the liquid, respectively, which coexist at a given temperature. The three sharp-kink profiles form a reference set against which the excess grand potential per unit area is measured. The same method was used by Groh and coworkers [43] to calculate the liquid/vapour surface tension of the restricted primitive model of an ionic solution. Note that due to the discontinuity of the auxiliary sharp kink profiles in eq. (51), the associated free energy $F [\{\rho_{\alpha}^{SK}(z)\}]$ is discontinuous at $z=0$, and takes on bulk values for $z<0$ (vapour) and for $z>0$ (liquid).

We have calculated the variation of the surface tension of the free liquid/vapour interface with ion concentration for several temperatures. A representative sample of the results we have obtained is shown in Fig. 7. γ_{lv} of the model solutions is significantly lower than that of real aqueous solutions at room temperature (about 70 mN/m). Such a result is not surprising, as our model does not account for the complex network of hydrogen bonds which form between water molecules, and which introduce a substantial contribution to its liquid/vapour surface tension. Contrary to the behaviour observed for alkali halides in water, our calculations show a slow but systematic decrease of γ_{lv} with ion concentration (as seen in the inset of Fig. 7). This trend was found to be true for both “semi-primitive” and “civilized” models. The main reason behind this disagreement is the poor description of electrostatic interactions in the bulk fluid within the mean-field approximation. The electrostatic contribution to the uniform fluid’s free energy vanishes identically, resulting in a phase diagram where the coexisting phases’ total densities are essentially independent of ion concentration (see Fig.1 of ref. [16]), unlike in real ionic solutions, where the total density of the liquid phase increases with c , leading to an increase in γ_{lv} . The actual decrease of $\gamma_{lv}(c)$ for our model solution is most likely related to the accumulation of chlorine anions (the largest species in the system) in the interfacial region. Such an entropic effect has been observed in dilute electrolytes, where the change in the total density of the solution is minor.

We have also investigated the solid/liquid surface tension γ_{sl} . This quantity is related to the inhomogeneous density profiles of an ionic solution under coexistence conditions in contact with a substrate by the following equation:

$$\gamma_{sl} = F [\{\rho_{\alpha}(z)\}] - F (\{\rho_{\alpha}^l\}) + \sum_{\alpha} \int_0^{\infty} [V_{\alpha}(z)\rho_{\alpha}(z) - \mu_{\alpha} (\rho_{\alpha}(z) - \rho_{\alpha}^l)] dz \quad (52)$$

As for the free liquid/vapour interface, we analysed the influence of ion concentration on surface tension, and compared $\gamma_{sl}(c)$ curves obtained for different dielectric permittivity models and substrate-fluid interaction parameters. Unlike $\gamma_{lv}(c)$, for the vast majority of systems investigated $\gamma_{sl}(c)$ is not a monotonic function and has a minimum. The location of this minimum depends on both the dielectric

properties of the solvent and the substrate-fluid potential. The typical variation of γ_{sl} with c is illustrated in Fig. 8. However, note that even if no minimum was found within the concentration range investigated, the system in question most likely has one at a lower c , since for very dilute solutions the amount of counterions needed to neutralise the substrate's charge is very high in comparison with this species' bulk density, which introduces a large contribution to the surface tension. Complete wetting occurs if the condition that $\gamma_{sv} = \gamma_{lv} + \gamma_{sl}$ is fulfilled. Therefore, our latest results for γ_{lv} and γ_{sl} indicate that the wetting transition temperature of an ionic solution near a charged substrate is generally a non-monotonic function of solute concentration.

8 Conclusions.

We have reviewed and supplemented recent theoretical work investigating the influence of dissolved monovalent ions on the wetting and drying scenarios of model solvents near a charged solid substrate.

The earlier approach is based on the primitive model representation of ionic solutions, and combines Cahn's square gradient DFT for the solvent with non-linear Poisson-Boltzmann theory of the ionic double-layers. Subsequent approaches use explicit solvent representations, and build on the classic DFT theory of Evans and collaborators for the wetting and drying behaviour of simple fluids. Ions have a small but significant effect on the wetting behaviour of ionic solutions, leading in particular to a shift of the wetting temperature. Close to the physical conditions where a cross-over from a first to a second order wetting transition is observed for the pure solvent, the addition of ions can change the order of the transition.

The predictions based on the "semi-primitive" model (with a local Clausius-Mossotti dielectric permittivity) are very close to those obtained with the "civilized" model using a mean-field description of the electrostatic interactions between ions and dipoles. Both models predict a novel drying transition which is completely absent in the pure solvent.

The new results for the surface tension γ_{lv} of the liquid-vapour interfaces predict a slow decrease of γ_{lv} with increasing ion concentration c , and a sharp drop with increasing temperature. The surface tension of the substrate-liquid interface, on the other hand, is found to have a minimum at a certain c_{min} . The variation pattern of the surface tension associated with these two types of interfaces indicates that wetting temperatures of ionic solutions are typically non-monotonic functions of the solute concentration c . The decrease of γ_{lv} as c increases is opposite to the trend observed experimentally for aqueous solutions, pointing to the expected failure of the "semi-primitive" and "civilized" solvent models to provide a realistic description of water. A DFT of wetting by aqueous ionic solutions, based on a realistic representation of water, e.g. the SPC/E [44] or the TIP4P [45] models, is not yet available, and should be a goal for future investigations. Another important objective for future work is an extension of the present DFT and of time-dependent density-functional theory (TDFT) [46] to explore the technologically important electro-wetting phenomena which are well documented experimentally [47].

Acknowledgements

We are indebted to Bob Evans and Roland Roth for their interest in our work. JPH would like to thank Bob Evans for constant inspiration over more than 30 years.

References

- [1] Heydweiller, A. *Ann. Phys. (Leipzig)* **338**, 145 (1910).
- [2] Wagner, V. C. *Phys. Zeitschrift* **25**, 474 (1924).
- [3] Onsager, L. and Samaras, N. N. T. *J. Chem. Phys.* **2**, 528 (1934).
- [4] Levin, Y. and Flores-Mena, J. E. *Europhys. Lett.* **56**, 187 (2001).
- [5] Bonn, D. and Ross, D. *Rep. Progr. Phys.* **64**, 1085 (2001).
- [6] de Gennes, P. G. *Rev. Mod. Phys.* **57**, 827 (1985).
Dietrich, S. In *Phase Transitions and Critical Phenomena*, Domb, C. and Lebowitz, J. L., editors, volume 12. Academic Press, London (1988).
- [7] Langmuir, I. *Science* **88**, 430 (1938).
- [8] Derjaguin, B. V. and Churaev, N. V. *J. Colloid Interface Sci.* **49**, 249 (1974).
- [9] Pashley, R. M. and Kitchener, J. A. *J. Colloid Interface Sci.* **71**, 491 (1979).
Pashley, R. M. *J. Colloid Interface Sci.* **78**, 246 (1980).
- [10] Kayser, R. F. *Phys. Rev. Lett.* **56**, 1831 (1986).
- [11] Evans, R. In *Fundamentals of Inhomogeneous Fluids*, Henderson, D., editor. Marcel Dekker, New York (1991).
- [12] Hansen, J.-P. and McDonald, I. R. *Theory of Simple Liquids*. Academic Press, Amsterdam, 3rd edition, (2006). Chap. 6.
- [13] Denesyuk, N. A. and Hansen, J.-P. *Europhys. Lett.* **63**, 261 (2003).
- [14] Denesyuk, N. A. and Hansen, J.-P. *J. Chem. Phys.* **121**, 3613 (2004).
- [15] Oleksy, A. and Hansen, J.-P. *Mol. Phys.* **104**, 2871 (2006).
- [16] Oleksy, A. and Hansen, J.-P. *Mol. Phys.* **107**, 2609 (2009).
- [17] Oleksy, A. and Hansen, J.-P. *J. Chem. Phys.* **132**, 204702 (2010).
- [18] Cahn, J. W. *J. Chem. Phys.* **66**, 3667 (1977).
- [19] Ebner, C. and Saam, W. F. *Phys. Rev. Lett.* **38**, 1486 (1977).
- [20] Sullivan, D. E., Levesque, D., and Weis, J. J. *J. Chem. Phys.* **72**, 1170 (1980).
- [21] Tarazona, P. and Evans, R. *Mol. Phys.* **52**, 847 (1984).
- [22] Sweatman, M. B. *Mol. Phys.* **98**, 573 (2000).
- [23] van der Waals, J. D. *Zeit. Phys. Chem.* **13**, 657 (1894).
- [24] Rowlinson, J. S. and Widom, B. *Molecular Theory of Capillarity*. Clarendon Press, Oxford, (1982).

- 1 [25] Sullivan, D. E. *Phys. Rev. B* **20**, 3991 (1979).
2
3 [26] Sullivan, D. E. *J. Chem. Phys.* **74**, 2604 (1981).
4
5 [27] Tarazona, P. and Evans, R. *Mol. Phys.* **48**, 799 (1983).
6
7 [28] Tarazona, P., Telo da Gama, M. M., and Evans, R. *Mol. Phys.* **49**, 283 (1983).
8
9 Tarazona, P., Telo da Gama, M. M., and Evans, R. *Mol. Phys.* **49**, 301 (1983).
10
11 [29] Tarazona, P., Marini Bettolo Marconi, U., and Evans, R. *Mol. Phys.* **60**, 573 (1987).
12
13 [30] Rosenfeld, Y. *Phys. Rev. Lett.* **63**, 980 (1989).
14
15 Rosenfeld, Y. *J. Chem. Phys.* **98**, 8126 (1993).
16
17 [31] Roth, R., Evans, R., Lang, A., and Kahl, G. *J. Phys. Cond. Matter* **14**, 12063 (2002).
18
19 [32] Roth, R. *J. Phys. Cond. Matter* **22**, 063102 (2010).
20
21 [33] Carnie, S. L. and Chan, D. Y. C. *J. Chem. Phys.* **73**, 2949 (1980).
22
23 [34] Augousti, A. T. and Rickayzen, G. *J. Chem. Soc. Faraday Trans. 2* **80**, 141 (1984).
24
25 [35] Tang, Z., Scriven, L. E., and Davis, H. T. *J. Chem. Phys.* **97**, 494 (1992).
26
27 [36] Zhang, L., Davis, H. T., and White, H. S. *J. Chem. Phys.* **98**, 5793 (1993).
28
29 [37] Biben, T., Hansen, J.-P., and Y., R. *Phys. Rev. E* **57**, R3727 (1998).
30
31 [38] Ghosal, S., Hemminger, J. C., Bluhm, H., Mun, B. S., Hebenstreit, E. L. D., Ketteler, G., Ogle-
32 tree, D. F., Requejo, F. G., and Salmeron, M. *Science* **307**, 563 (2005).
33
34 [39] Jungwirth, P. and Tobias, D. J. *J. Phys. Chem. B* **105**, 10468 (2001).
35
36 [40] Jungwirth, P. and Tobias, D. J. *J. Phys. Chem. B* **106**, 6361 (2002).
37
38 [41] Teixeira, P. I. and Telo da Gama, M. M. *J. Phys. Cond. Matter* **3**, 111 (1991).
39
40 [42] Frodl, P. and Dietrich, S. *Phys. Rev. A* **45**, 7330 (1992).
41
42 [43] Groh, B., Evans, R., and Dietrich, S. *Phys. Rev. E* **57**, 6944 (1998).
43
44 [44] Berendsen, H. J. C., Grigera, J. R., and Straatsma, T. P. *J. Phys. Chem.* **91**, 6269 (1987).
45
46 [45] Abascal, J. L. and Vega, C. *J. Chem. Phys.* **123**, 234505 (2005).
47
48 [46] Marini Bettolo Marconi, U. and Tarazona, P. *J. Chem. Phys.* **110**, 8032 (1999).
49
50 [47] Mugele, F. and Baret, J.-C. *J. Phys. Cond. Matter* **17**, R705 (2005).
51
52
53
54
55
56
57
58
59
60

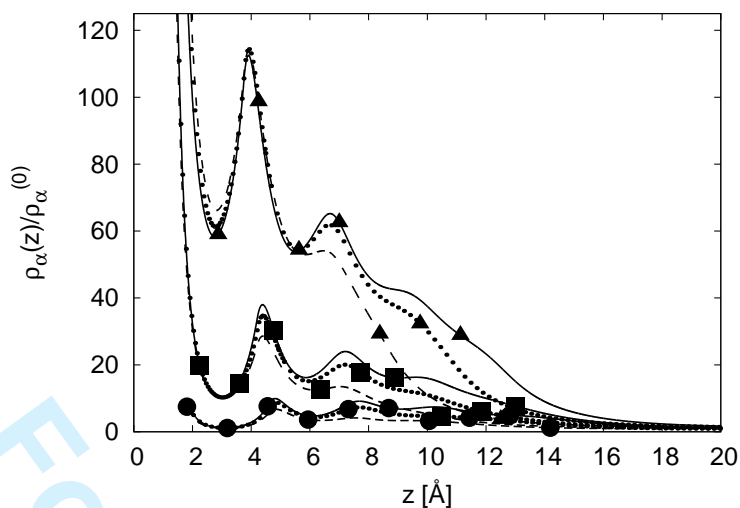


Figure 1: Density profiles $\rho_\alpha(z)$ formed by NaCl vapour in contact with a charged substrate, illustrating the liquid film growth as coexistence conditions are approached along an isotherm. The saturated vapour coexists with a 0.1M solution. The dashed lines correspond to $\rho_\alpha^{(0)} = 0.99\rho_\alpha^{\text{co}}$, dotted lines to $\rho_\alpha^{(0)} = 0.999\rho_\alpha^{\text{co}}$ and solid lines to $\rho_\alpha^{(0)} = 0.9999\rho_\alpha^{\text{co}}$. Na^+ (counterion) profiles are marked with triangles, Cl^- (coion) profiles with circles, and H_2O profiles with squares. $\epsilon(z)$ is approximated using a sigmoidal function mimicking the permittivity of water (eq. (34) from ref. [16]), $k_w = k_f = 1.8$, $\sigma^* = -0.022$, $T^* = 0.736$.

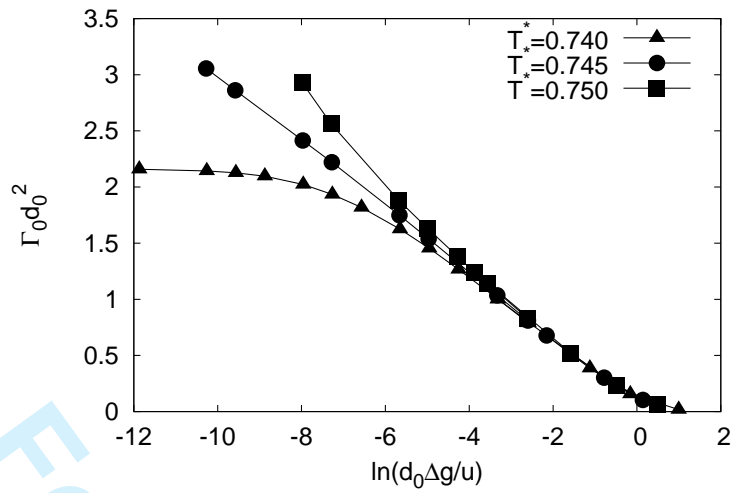


Figure 2: Adsorption of the SPM solvent as a function of distance from coexistence along three isotherms in the vicinity of a second order wetting transition ($T_w^* \simeq 0.744$) for dimensionless inverse range parameters $k_w = k_f = 1.8$. The saturated vapour coexists with a 0.1M NaCl solution. The dielectric permittivity is given by eq. (37). The substrate is uncharged.

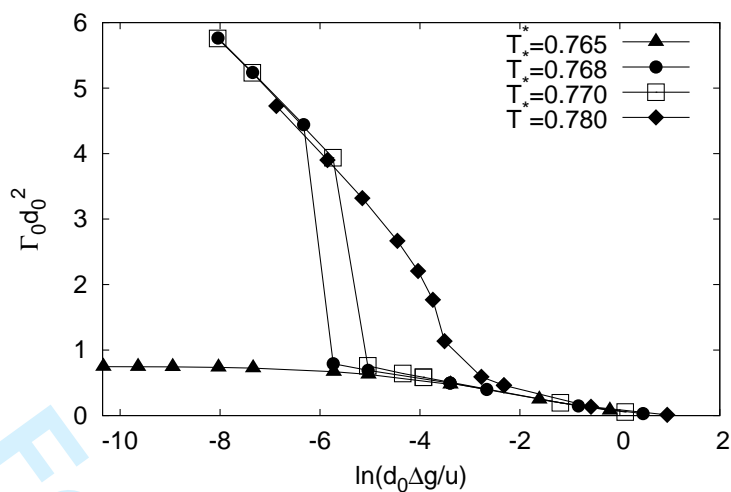


Figure 3: Same as in Fig. 2, but for $k_w = 1.2$, and four isotherms. The wetting transition in this system is first order and occurs at $T_w^* \simeq 0.766$.

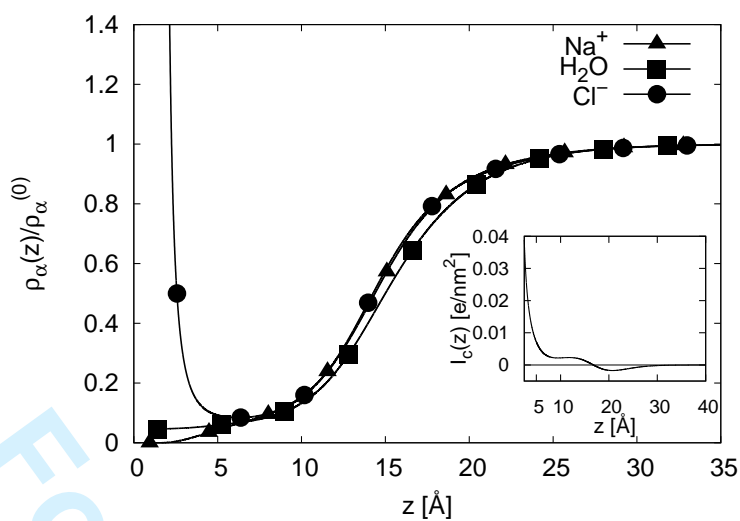


Figure 4: Density profiles of 1M NaCl at liquid-vapour coexistence near a hard wall carrying a surface charge $\sigma^* = +0.0087$. $T^* = 0.75$, $\epsilon(z)$ is the CM function defined by (37). The inset shows the total amount of charge per unit area $I_c(z)$ contained between 0 and z (including the substrate charge).

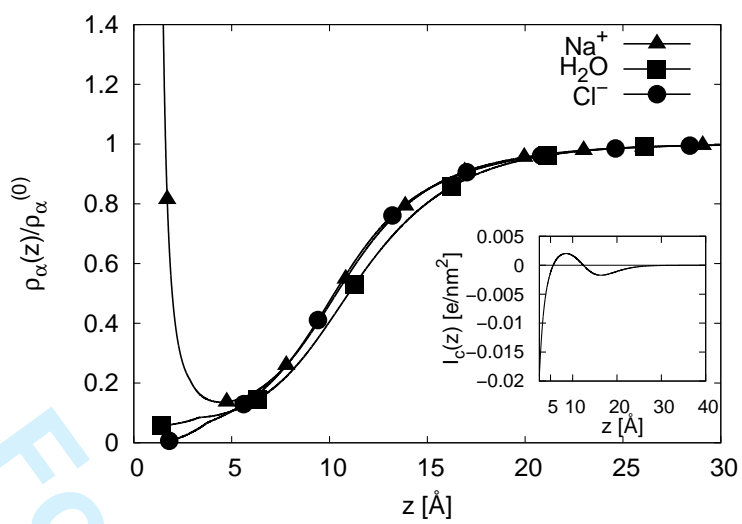


Figure 5: As in Fig. 4, but for $\sigma^* = -0.072$.

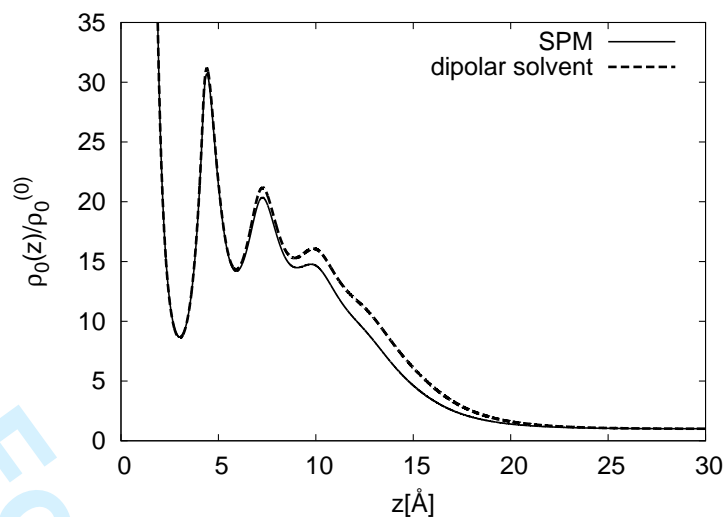


Figure 6: Solvent density profiles at coexistence (gas branch) compared for the SPM (with CM permittivity (37)) and the “civilized” solution model. The NaCl concentration in the corresponding liquid phase is 0.1M. The vapour is in contact with a wall carrying a surface charge density $\sigma^* = +0.022$ and exerting an exponential attraction with an inverse range parameter $k_w = 1.8$. The temperature $T^*=0.743$ and the reduced dipole moment $m^*=0.75$. Both systems are close to a second order wetting transition.

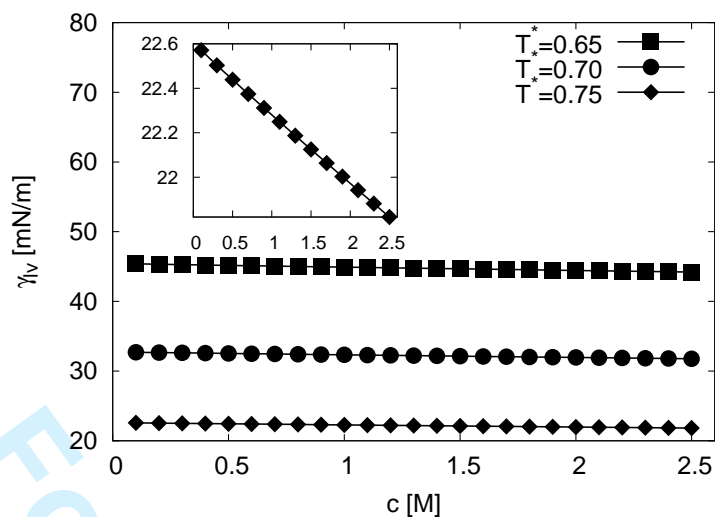


Figure 7: The liquid-vapour surface tension of SPM NaCl solutions as a function of ion concentration. The inset shows a single curve corresponding to $T^* = 0.75$ to illustrate the steady decrease of γ_{lv} with c . $\varepsilon(z)$ is approximated using a sigmoidal function mimicking the permittivity of water.

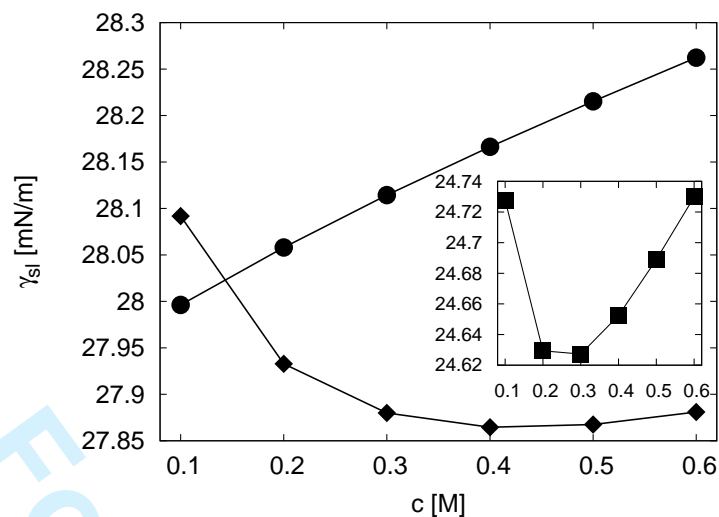


Figure 8: The liquid-vapour surface tension of SPM NaCl solutions as a function of ion concentration. For all systems illustrated in this figure $k_w = 1.2$, and $T^* = 0.77$. The line marked with circles corresponds to $\sigma^* = -0.022$ and sigmoidal $\varepsilon(z)$ as in Fig. 1 (values of ε in the liquid are close to 80, as in real water), the line marked with diamonds to identical σ^* , but $\varepsilon(z)$ given by the CM formula (with $m^* = 0.75$, which yields liquid phase permittivity about 10 times smaller than the sigmoidal formula), and the line marked with squares (shown in the inset for clarity) to $\sigma^* = -0.043$ and sigmoidal $\varepsilon(z)$.